Improvement performances of Doubly Fed Induction Generator via MPPT Strategy using Model Reference Adaptive Control based Direct Power Control with Space Vector Modulation

F. AMRANE[1], A. CHAIBA[1], A. CHEBABHI[2]
[1]LAS Research Laboratory, Setif 1University, Algeria.
[2]ICEPS Laboratory, Department of Electrical Engineering, Djillali Liabes University
E-mail : amrane_fayssal@live.fr

Abstract— *In this paper Model Reference Adaptive Control (MRAC) for Wind energy conversion system (WECS) doubly fed induction generator (DFIG) is proposed using direct power control (DPC) based on space-vector modulation (SVM) afor fixed switching frequency in the d-q reference frame is proposed for wind generation application using MPPT strategy. First, a mathematical model of the doubly-fed induction generator written in an appropriate d-q reference frame is established to investigate simulations. In order to control the DFIG direct power control and space-vector modulation (DPC-SVM) are combined to replace the hysteresis controllers used in the original DPC drive, the active and reactive powers are controllers by a PID regulators. The performances of MRAC which is based on the DPC-SVM combination are investigated and compared to those obtained from the PID regulators Results obtained in Matlab/Simulink® environment show that the MRAC is more robust, superior dynamic performance and hence found to be a suitable replacement of the conventional controller for the high performance drive applications.*

Keywords— *Model reference adaptive control (MRAC), Wind energy conversion system (WECS), Doubly fed induction generator (DFIG), Direct power control (DPC), Space vector modulation (SVM), Maximum power point tracking (MPPT).*

1. Introduction

Wind energy conversion system (WECSs) based on the doubly fed induction generator (DFIG) dominated the wind power generations due to the outstanding advantages, including small converters rating around 30% of the generator rating, lower converter cost. Several novel control strategies have been investigated in order to improve the DFIG operation performance [1-2]. Nowadays, since DFIG-based WECSs are mainly installed in remote and rural areas [2]. In literature [3] vector control is the most popular method used in the DFIG-based wind turbines. The DPC is simple and alternative approach control formulation that does not require decomposition into symmetrical components; the DPC schemes have been proved to be preponderant for DFIGs due to the simple implementation [4]. A new modeling approach based on independent from the flux measurement has been proposed in [5], in order to conclude input-to-state stability and convergence to the desired equilibrium. In [6] the direct power control (DPC) of a single voltage source converter based on doubly fed induction generator (DFIG) without using a rotor position sensor. Simulation and experimental results of a 3.7 kW DFIG system are presented to demonstrate the performance of the proposed WECS under steady state.

A schematic diagram of wind turbine system with a DFIG is shown in figure 1.

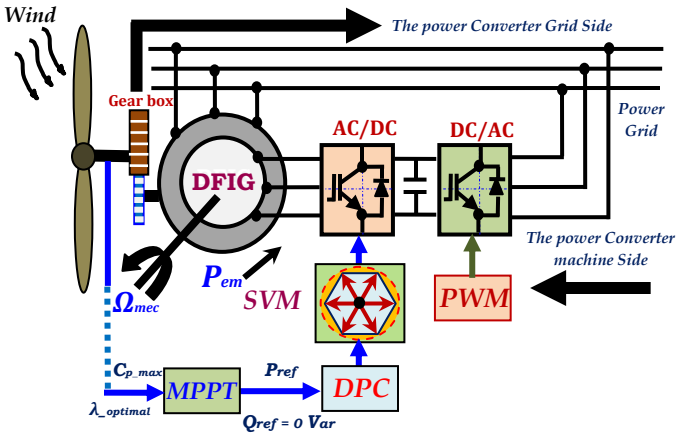

Fig. 1. Schematic diagram of wind turbine system with a DFIG.

Control strategies of DFIG have been discussed in details in literatures; Direct Power Control (DPC) [5-6], Model

Predictive Direct Power Control (MPDPC) [7-8], Sliding mode Direct Power Control [9], Sliding mode control [10-11] and Backstepping Control [12].

The maximum power point tracking (MPPT) strategy takes big importance in last researches, as in [13] the authors propose a modified perturbation and observation (P&O) maximum power point tracking (MPPT) algorithm in order to improve the divergence from peak power and the rapidity/efficiency trade-off under a fast variation of the wind speed for small WECSs.

In [14] the authors have presented a model reference adaptive control (MRAC) speed estimator for speed sensorless direct torque and flux control of an induction motor, to achieve high performance sensorless drive. Other advantages of MRAC are it has the ability to control the system that undergoes parameter and/or environmental variations. This is based on advantages of MRAC in which the desired transient specification is given in terms of reference model so that it's give selectivity to designers to set the desired transient performance by adjusting the reference model either to have fast or slow transient output.

In this paper, MRAC is used for adjusting rotor current of DFIG. This paper is organized as follows; firstly the modeling of the turbine is presented in section 2. In section 3, the mathematical model of DFIG is given. Section 4 presents Direct Power Control of DFIG which is based on the orientation of the stator flux vector along the axe 'd'. In section 5 the Model Reference Adaptive Control (MRAC) is established to control the rotor currents after being compared by conventional regulators PID. In section 6, computer simulation results are shown and discussed. Finally, the reported work is concluded in section 7.

2. Model of the Turbine

The wind turbine input power usually is:

$$P_v = \frac{1}{2} * \rho * S_w * v^3 \quad (1)$$

Where ρ is air density; S_w is wind turbine blades swept area in the wind; v is wind speed.

The output mechanical power of wind turbine is:

$$P_m = C_p * P_v = \frac{1}{2} * C_p * \rho * S_w * v^3 \quad (2)$$

Where C_p represents the wind turbine power conversion efficiency. It is a function of the tip speed ratio λ and the blade pitch angle β in a pitch-controlled wind turbine. λ is defined as the ratio of the tip speed of the turbine blades to wind speed. λ is given by:

$$\lambda = \frac{R*\Omega_t}{v} \quad (3)$$

Where R is blade radius, Ω_t is angular speed of the turbine. C_p can be described as [15]:

$$C_p = \left(0.5 - 0.0167 * (\beta - 2)\right) * \sin\left[\frac{\pi*(\lambda+0.1)}{18.5-0.3*(\beta-2)}\right] - 0.00184 * (\lambda - 3) * (\beta - 2) \quad (4)$$

The maximum value of Cp ($C_{p\_max} = 0.4785$) is achieved for $\beta = 0$ degree and for $\lambda_{opt} = 8.107$. This point corresponds at the maximum power point tracking (MPPT).

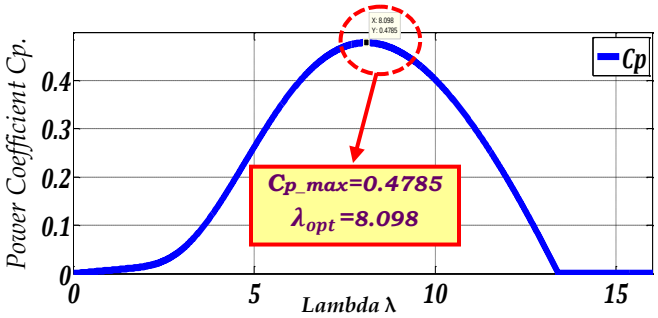

Fig. 2. Aerodynamic power coefficient variation Cp against tip speed ratio λ and pitch angle β.

In our work we use the wind profile, as shown in Fig.3:

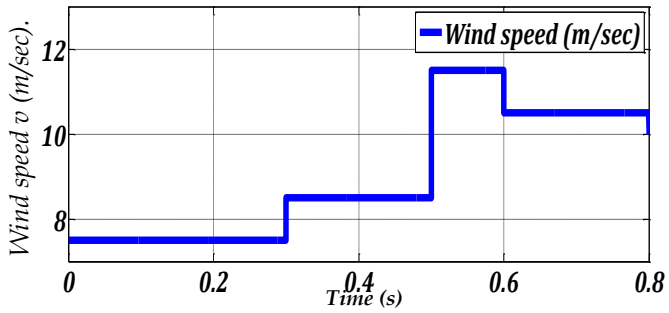

Fig. 3. Wind profile (Wind Speed).

After the simulation of the wind turbine using this wind profile, we test the robustness of our MPPT algorithm, we have as results the curve of power coefficient Cp versus time; this latter achieved the maximum value mentioned in Fig.2 ($C_{p\_max} = 0.4785$) despite the variation of the wind

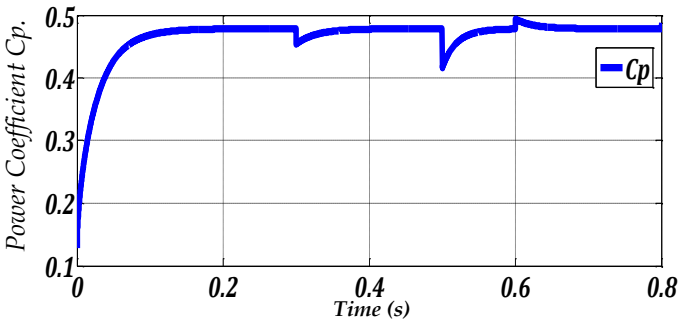

Fig. 4. Power coefficient (Cp).

3. Mathematical Model of DFIG

The generator chosen for the conversion of wind energy is a double-fed induction generator, DFIG modeling described in the two-phase reference (Park). The general electrical state model of the induction machine obtained using Park transformation is given by the following equations, [16-20]:

Stator and rotor voltages:

$$V_{sd} = R_s * i_{sd} + \frac{d}{dt}\emptyset_{sd} - \omega_s * \emptyset_{sq} \quad (5)$$

$$V_{sq} = R_s * i_{sq} + \frac{d}{dt}\emptyset_{sq} + \omega_s * \emptyset_{sd}. \quad (6)$$

$$V_{rd} = R_r * i_{rd} + \frac{d}{dt}\emptyset_{rd} - (\omega_s - \omega) * \emptyset_{rq} \quad (7)$$

$$V_{rq} = R_r * i_{rq} + \frac{d}{dt}\emptyset_{rq} + (\omega_s - \omega) * \emptyset_{rd} \quad (8)$$

Stator and rotor fluxes:

$$\emptyset_{sd} = L_s * i_{sd} + L_m * i_{rd} \quad (9)$$

$$\emptyset_{sq} = L_s * i_{sq} + L_m * i_{rd} \quad (10)$$

$$\emptyset_{rd} = L_r * i_{rd} + L_m * i_{sd} \quad (11)$$

$$\emptyset_{rq} = L_r * i_{rq} + L_m * i_{sq} \quad (12)$$

The electromagnetic torque is given by:

$$C_e = P * L_m * (i_{rd} * i_{sq} - i_{rq} * i_{sd}) \quad (13)$$

And its associated motion equation is:

$$C_e - C_r = J * \frac{d}{dt}\Omega + f * \Omega \quad (14)$$

$$J = \frac{J_{turbine}}{G^2} + J_g \quad (15)$$

Where: C_r is the load torque J is total inertia in DFIG's rotor, Ω is mechanical speed and G is gain of gear box.

The voltage vectors, produced by a three-phase PWM inverter, divide the space vector plane into six sectors, as shown in Fig. 5 [15].

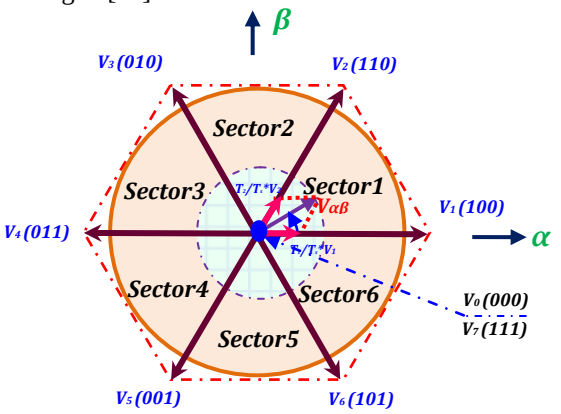

Fig. 5. The diagram of voltage space vectors in *α-β* plan.

In every sector, each voltage vector is synthesized by the basic space voltage vector of the 2 sides of the sector and 1 zero vector. For example, in the first sector, $V_{\alpha\beta}$ are the synthesized voltage space vector and are expressed by:

$$\vec{V}_{\alpha\beta} = \frac{T_1}{T_S} * \overrightarrow{V_1} + \frac{T_2}{T_S} * \overrightarrow{V_2} \quad (16)$$

After projection of the vectors $V_{\alpha\beta}$, V_α and V_β we have:

$$V_\alpha = \|\vec{V}_{\alpha\beta}\| * \cos(\theta) = \frac{T_1}{T_S} * \left(\frac{\sqrt{2}}{\sqrt{3}} * V_{dc}\right) + \frac{T_2}{T_S} * \left(\frac{\sqrt{2}}{\sqrt{3}} * V_{dc}\right) * \cos\frac{\pi}{3} \quad (17)$$

$$V_\beta = \|\vec{V}_{\alpha\beta}\| * \sin(\theta) = \frac{T_2}{T_S} * \left(\frac{\sqrt{2}}{\sqrt{3}} * V_{dc}\right) * \sin\frac{\pi}{3} \quad (18)$$

$$T_1 = \frac{(\sqrt{6} * V_\alpha - \sqrt{2} * V_\beta)}{2 * V_{dc}} * T_S \quad (19)$$

$$T_2 = \frac{\sqrt{2} * V_\beta}{V_{dc}} * T_S \quad (20)$$

4. Direct Power Control of DFIG

In this section, the DFIG model can be described by the following state equations in the synchronous reference frame whose axis *d* is aligned with the stator flux vector as shown in Fig. 6, ($\emptyset_{sd} = \emptyset_s$)and ($\emptyset_{sq} = 0$) [17].

By neglecting resistances of the stator phases the stator voltage will be expressed by:

$$V_{sd} = 0 \; and \; V_{sq} = V_s \cong \omega_s * \emptyset_s \quad (21)$$

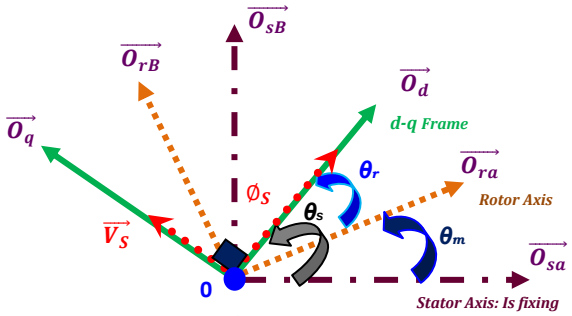

Fig. 6. Stator and rotor flux vectors in the synchronous d-q Frame.

We lead to an uncoupled power control; where, the transversal component i_{rq} of the rotor current controls the active power. The reactive power is imposed by the direct component i_{rd} as in shown in Fig. 7:

$$P_s = -V_s * \frac{L_m}{L_s} * i_{rq} \quad (22)$$

$$Q_s = \frac{V^2{}_s}{\omega_s * L_s} - V_s * \frac{L_m}{L_s} * i_{rd} \quad (23)$$

The arrangement of the equations gives the expressions of the voltages according to the rotor currents as in shown in Fig. 8:

$$V_{rd} = R_r * i_{rd} + \left(L_r - \frac{L_m^2}{L_s}\right) * \frac{di_{rd}}{dt} - g * \omega_s * \left(L_r - \frac{L_m^2}{L_s}\right) * i_{rq} \quad (24)$$

$$V_{rq} = R_r * i_{rq} + \left(L_r - \frac{L_m^2}{L_s}\right) * \frac{di_{rq}}{dt} + g * \omega_s * \left(L_r - \frac{L_m^2}{L_s}\right) * i_{rd} + g * \frac{L_m * V_s}{L_s} \quad (25)$$

$$i_{rd} = -\frac{1}{\sigma * \tau_r} * i_{rd} + g * \omega_s * i_{rq} + \frac{1}{\sigma * L_r} * V_{rd} \quad (26)$$

$$i_{rq} = -\frac{1}{\sigma}\left(\frac{1}{\tau_r} + \frac{L_m^2}{L_s * T_s * L_r}\right) * i_{rq} - g * \omega_s * i_{rd} + \frac{1}{\sigma * L_r} * V_{rq} \quad (27)$$

with:

$$T_r = \frac{L_r}{R_r};\; T_s = \frac{L_s}{R_r};\; \sigma = 1 - \frac{L_m^2}{L_s * L_r} \quad (28)$$

where: ϕ_{sd}, ϕ_{sq} are stator flux components, ϕ_{rd}, ϕ_{rq} are rotor flux components, V_{sd}, V_{sq} are stator voltage components, V_{rd}, V_{rq} are rotor voltage components. R_s, R_r are stator and rotor resistances, L_s, L_r are stator and rotor inductances, L_m is mutual inductance, σ is leakage factor, P is number of pole pairs, $\omega_s$is the stator pulsation, ω is the rotor pulsation, f is the friction coefficient, T_s and T_r are stator and rotor time-constant, and g is the slid.

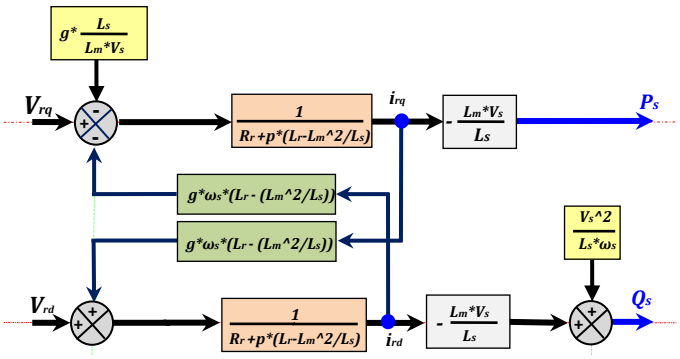

Fig. 7. The Doubly Fed Induction Generator simplified model.

5. Model Reference Adaptive Control (MRAC)

The system studied in this paper is based on a first-order linear plant approximation given by [18]:

$$\dot{x}(t) = -a.x(t) + b.u(t) \tag{29}$$

Where x(t) is the plant state, u(t) is the control signal and a and b are the plant parameters. The control signal is generated from both the state variable and the reference signal r(t), multiplied by the adaptive control gains K and Kr such that

$$u(t) = K(t).x(t) + K_r(t).r(t) \tag{30}$$

Where $K(t)$ is the feedback adaptive gain and $Kr(t)$ the feed forward adaptive gain. The plant is controlled to follow the output from a reference model

$$\dot{x_m}(t) = a_m x_m(t) + b_m r(t) \tag{31}$$

Where x_m is the state of the reference model and a_m and b_m are the reference model parameters which are specified by the controller designer. The object of the $MRAC$ algorithm is for $x_e \rightarrow 0$ as $t \rightarrow \infty$, where $x_e = x_m - x$ is the error signal. The dynamics of the system may be rewritten in terms of the error such that

$$\dot{x_e}(t) = a_m x_e(t) + \big(a - a_m - bK(t)\big)x(t) + (b_m - bK_r(t))r(t) \tag{32}$$

Using Equations (27), (28) and (29), it can be seen that for exact matching between the plant and the reference model, the following relations hold

$$K = K^E = \frac{a - a_m}{b} \tag{33}$$

$$K_r = K_r^E = \frac{b_m}{b} \tag{34}$$

Where $()^E$ denotes the (constant) Erzberger gains [19].

Equations (30) and (31) can be used to express Equation (29) as:

$$\dot{x_e}(t) = -a_m x_e + b(K^E - K).(x_m - x_e) + b(K^E - K).r \tag{35}$$

For general model reference adaptive control, the adaptive gains are commonly defined in a proportional plus integral formulation

$$K(e,t) = \int_0^t \alpha \,.\, y_e . I_{rdq}^T . dt + \beta . y_e . I_{rdq}^T \tag{36}$$

$$K_r(e,t) = \int_0^t \alpha \,.\, y_e . I_{rdqref}^T . dt + \beta . y_e . I_{rdqref}^T \tag{37}$$

Where α and β are adaptive control weightings representing the adaptive effort. y_e is a scalar weighted function of the error state and its derivatives, $y_e = C_e.x_e$, where C_e can be chosen to ensure the stability of the feed forward block.

The equivalent scheme of MRAC for adjusting rotor currents of DPC in this work is shown in Fig 9.

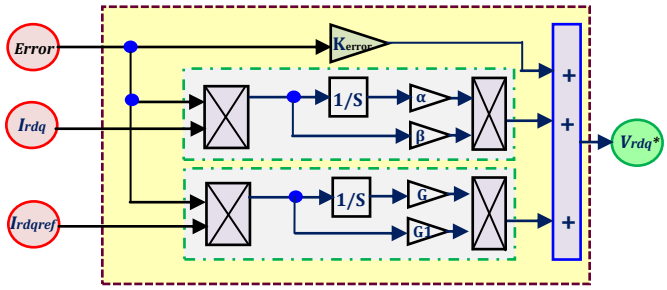

Fig. 9. The Simulink scheme of MRAC for rotor currents.

The proposed DPC of a DFIG based on MRAC is shown in fig.10.

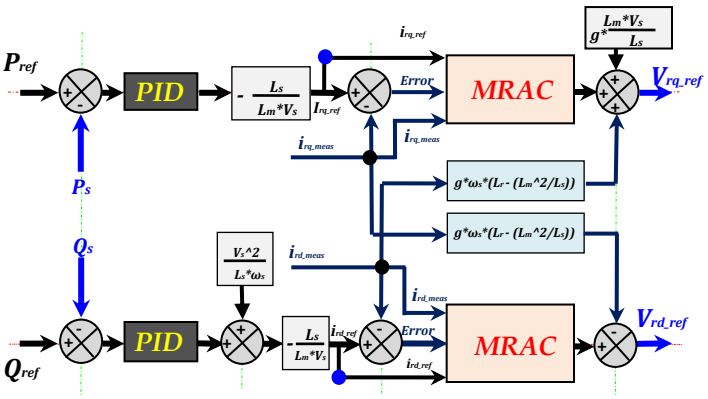

Fig. 8. Active and Reactive Power Control of a DFIG.

The overall system is described in detail, as shown in fig.10.

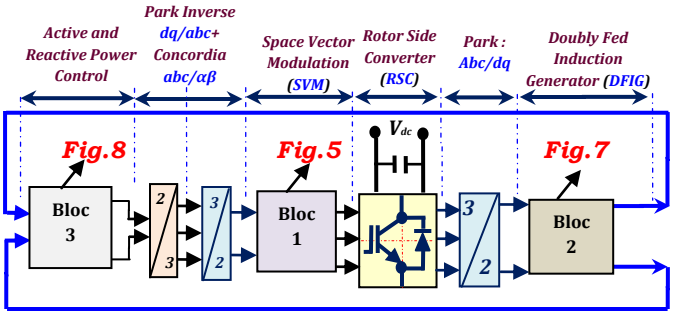

Fig. 10. Global System.

6. Simulation Results

DFIG used in this work is a *4kW* whose nominal parameters are indicated in Table.1. And the wind turbine used in this work is a *10 kW* whose parameters are indicated in Table.2.

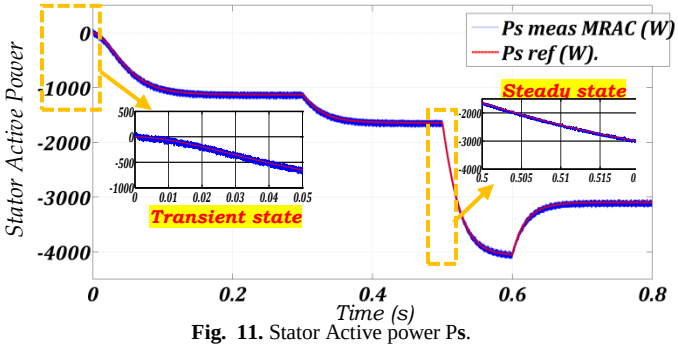

Fig. 11. Stator Active power Ps.

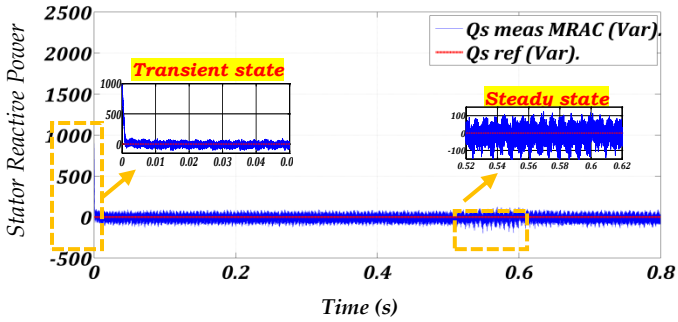

Fig. 12. Stator Reactive power QS.

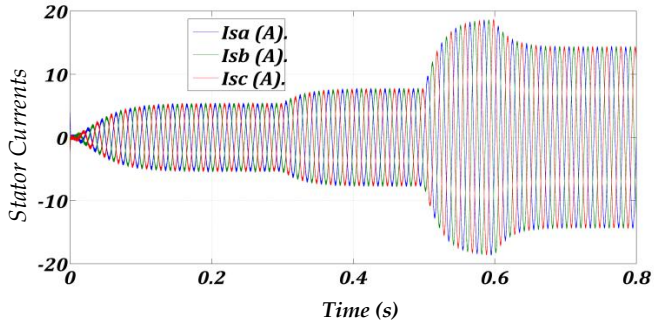

Fig. 13. Stator Currents Is_abc.

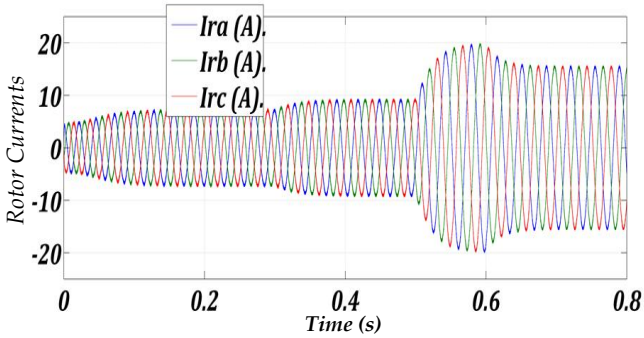

Fig. 14. Rotor Currents Ir_abc.

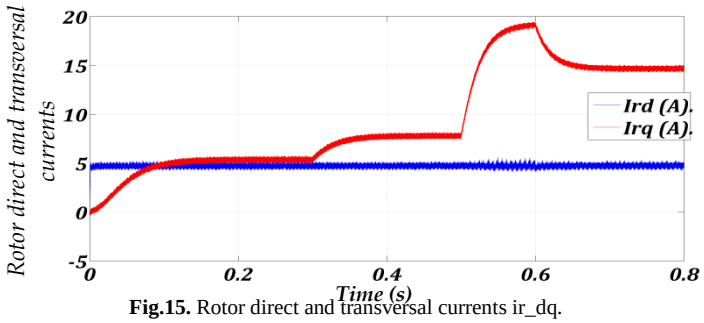

Fig.15. Rotor direct and transversal currents ir_dq.

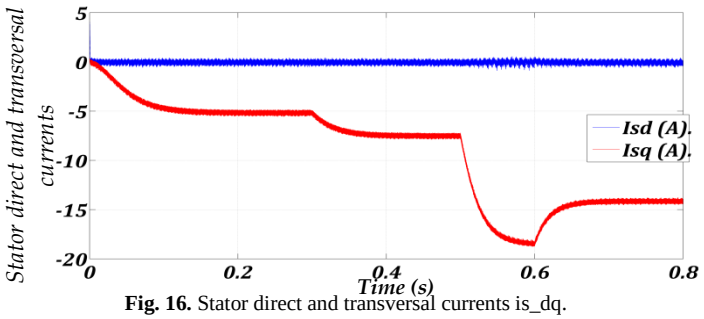

Fig. 16. Stator direct and transversal currents is_dq.

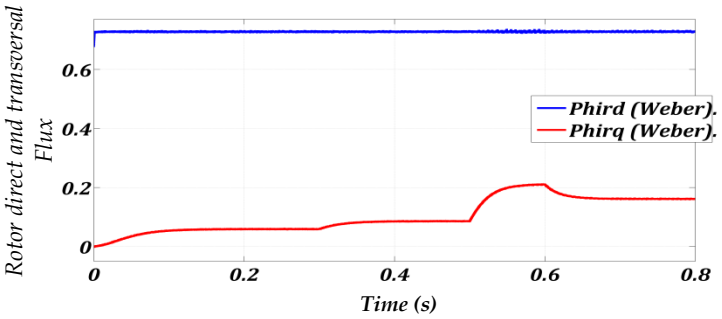

Fig. 17. Rotor direct and transversal flux ϕr_dq.

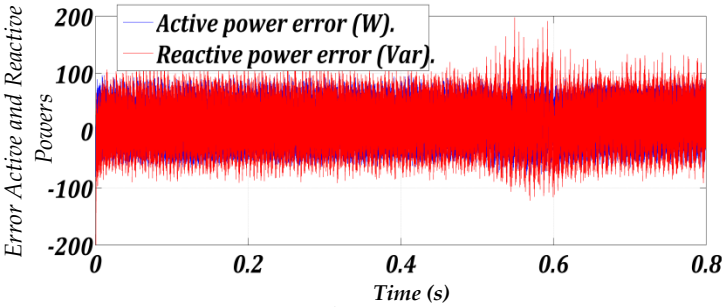

Fig. 18. Tracking errors of stator active and reactive powers.

Fig.11 presents the stator active power and its reference profiles injected into the grid using SVM, the stator active power reference is extracted from MPPT strategy. The stator reactive power and its reference profiles using SVM are presented in Fig.12, represent power factor unity equal to 0Var. It is clear that the measure powers (active and reactive) have good chase with high performance (little error, and short response time) as for as their reference powers.

Fig.13 represents the stator current i_{s_abc}, we remark the sinusoidal form of the three phases rotor currents.

Fig.14 shows the rotor current i_{r_abc}, we observe the sinusoidal form of the three phases stator currents.

Fig.15 shows the rotor direct current and the rotor transversal current respectively. We remark that the rotor direct and transversal currents have the inverse diagrams as for as reactive and active power.

Fig.16 shows the stator direct current and the stator transversal current. We observe that the stator direct and transversal currents have the same diagrams of reactive and active power respectively, so they represent the images of reactive and active power respectively.

Fig.17 shows the rotor direct flux and the rotor transversal flux. They represent the inverse diagrams of reactive and active power respectively.

Fig.18 shows the tracking errors of active and reactive powers. We observe a low error of active and reactive power nearly: $-100W/Var \leq \Delta Ps\_\Delta Qs \leq +100W/Var$. Except between 0.52 and 0.62 sec nearly $-150W/Var \leq \Delta Ps\_\Delta Qs \leq +150W/Var$

TABLE.1. PARAMETERS OF THE DFIG.

Rated Power:	*4 kWatts*
Stator Resistance:	*Rs = 1.2Ω*
Rotor Resistance:	*Rr = 1.8Ω*
Stator Inductance:	*Ls = 0.1554 H.*
Rotor Inductance:	*Lr = 0.1558 H.*
Mutual Inductance:	*Lm = 0.15 H.*
Rated Voltage:	*Vs = 220/380 V*
Number of Pole pairs:	*P= 2*
Rated Speed:	*N=1440 rpm*
Friction Coefficient:	f_{DFIG}*=0.00 N*m/sec*
The moment of inertia	*J=0.2 kg*m^2*
Slid:	*g=0.015*

TABLE.2. PARAMETERS OF THE TURBINE.

Rated Power:	*10 kWatts*
Number of Pole pairs:	*P= 3*
Blade diameter	*R= 3m*
Gain:	*G=3.9*
The moment of inertia	*Jt=0.00065 kg*m^2*
Friction coefficient	*ft=0.017 N*m/sec*
Air density:	*ρ=1.22 Kg/m^3*

7. Conclusion

In this paper Model Reference Adaptive Control for doubly fed induction generator (DFIG) based direct power control with a SVM has been proposed for wind generation application. Direct power control with MPPT strategy has been achieved by adjusting active and reactive powers and rotor currents. The performances of MRAC which is based on the DPC algorithm has been investigated and compared to those obtained from the PID controller. Simulation results obtained in $Matlab/\ Simulink^{®}$ have shown that the MRAC is more robust, lower errors, short response time and superior dynamic performance.

8. References

[1] H. Nian, Y. Song, "Direct Power Control of Doubly Fed Induction Generator under Distorted Grid Voltage", IEEE Transactions on Power Electronics, Vol. 29, No. 2,pp: 894 - 905, 2014.

[2] H. Nian, P. Cheng1, Z-Q. Zhu, "Coordinated Direct Power Control of DFIG System without Locked Loop under Unbalanced Grid Voltage Conditions", IEEE Transactions on Power Electronics, Vol. 31, No. 4,pp: 2905 – 2918, 2015.

[3] J. Mohammadi, S-V. Zadeh, S. Afsharnia, E. Daryabeigi, "A Combined Vector and Direct Power Control for DFIG-Based Wind Turbines", IEEE Transactions On Sustainable Energy, Vol. 5, No. 3,pp: 767 – 775, 2014.

[4] M-M. Baggu, B-H. Chowdhury, J-W. Kimball, "Comparison of Advanced Control Techniques for Grid Side Converter of Doubly-Fed Induction Generator Back-to-Back Converters to Improve Power Quality Performance During Unbalanced Voltage Dips", IEEE Journal Of Emerging And Selected Topics In Power Electronics, Vol. 03, No. 2,pp: 516 – 524, 2015.

[5] M-K. Bourdoulis, A-T. Alexandridis. "Direct Power Control of DFIG Wind Systems Based on Nonlinear Modeling and Analysis", IEEE Journal of Emerging and Selected Topics in Power Electronics, Vol. 2, No. 4,pp: 764 – 775, 2014

[6] B. Singh, N. K- Naidu, "Direct Power Control of Single VSC-Based DFIG without Rotor Position Sensor", IEEE Transactions On Industry Applications, Vol. 50, No. 6, pp: 4152 - 4163, 2014.

[7] J. Hu, J. Zhu, D-G. Dorrell, "Predictive Direct Power Control of Doubly Fed Induction Generators Under Unbalanced Grid Voltage Conditions for Power Quality Improvement", IEEE Transactions on Sustainable Energy, Vol. 6, No. 3, pp: 943 – 950, 2015.

[8] J. Hu, J. Zhu, D-G. Dorrell, "Model-predictive direct power control of doubly-fed induction generators under unbalanced grid voltage conditions in wind energy applications", IET Renewable Power Generation, vol. 8, pp. 687-695, pp: 687 – 695, 2014.

[9] E.G. Shehata, "Sliding mode direct power control of RSC for DFIGs driven by variable speed wind turbines", Alexandria Engineering Journal, Vol. 54, No. 4, pp: 1067 – 1075, 2015.

[10] S. Taraft , D. Rekioua, D. Aouzellag, S. Bacha, "A proposed strategy for power optimization of a wind energy conversion system connected to the grid", Energy Conversion and Management, Vol. 101, No. 1, pp: 489–, 2015.

[11] M. Doumi, A-G. Aissaoui, A. Tahour, M. Abid, "Commande Adaptative D'un Système Éolien", Rev. Roum. Sci. Techn. Électrotechn. Et Énerg, Vol. 60, No. 1, pp: 99–110, 2015.

[12] B. Bossoufi, M. Karim, A. Lagrioui, M. Taoussi, A. Derouich, "Observer backstepping control of DFIG-Generators for wind turbines variable-speed: FPGA-based implementation", Renewable Energy, Vol. 81, No. C, pp: 903-, 2015.

[13] Y. Daili, J.-P. Gaubert, L. Rahmani, "Implementation of a new maximum power point tracking control strategy for small wind energy conversion systems without mechanical sensors", Energy Conversion and Management. Vol. 97, pp. 298–306, 2015

[14] T. Ramesh n, A-K. Panda, S-S. hivaKumar, "Type-2 fuzzy logic control based MRAS speed estimator for speed sensorless direct torque and flux control of an induction motor drive", ISATransactions Vol. 57, pp: 262–275, 2015.

[15] Y. Bekakra, D-B. Attous, “DFIG Sliding Mode Control Driven by Wind Turbine with Using a SVM Inverter for Improve the Quality of Energy Injected into the Electrical Grid”, ECTI transactions on electrical Eng, electronics, and communications, Vol.11, No.1, pp: 36-75, 2013.

[16] G. Abad, J. Lopez, M-A. Rodrıguez, L. Marroyo, G. Iwanski, “Doubly fed induction machine: modeling and control for wind energy generation”, IEEE press Series on Power Engineering, ISBN: 978-0-470-76865-5, 2011.

[17] Y. Lei, A. Mullane, G. Lightbody, R. Yacamini, “Modeling of the wind turbine with a doubly-fed induction generator for grid integration studies”, IEEE Trans. Energy Conversion, Vol.21, No.1, pp: 257-264, 2006.

[18] K-J. Astrom, , B. Wittenmark, “Adaptive Control”. Addison Wesley, 1995.

[19]H-K. Khalil, “Nonlinear systems” Macmillan, New York, 1992.

[20] A. Chaiba, R. Abdessemed, M. L. Bendaas, A. Dendouga “Performances Of Torque Tracking Control For Doubly Fed Asynchronous Motor Using Pi And Fuzzy Logic Controllers”. Journal of Electrical Engineering, 2005.